A TAXONOMY OF WRINKLE RIDGES ON MARS. J. C. Andrews-Hanna[1] (Lunar and Planetary Laboratory, University of Arizona, Tucson, AZ 85721, jcahanna@lpl.arizona.edu).

Introduction: Wrinkle ridges are among the most common tectonic landforms in the Solar System, being abundant on the volcanic plains of the Moon, Mars, Mercury, and Venus. Wrinkle ridges provide an important tectonic record of strain related to both volcanic loading [1] and global cooling and contraction [2]. While the general model of folding above a blind thrust fault [3] is widely accepted, a number of key questions remain unanswered. There continues to be debate regarding whether or not wrinkle ridges are deeply penetrating lithosphere-scale faults [4, 5], whether the faults transition to horizontal décollements at depth, and the dip and arrangement of faults. Moreover, the term "wrinkle ridge" encompasses a vast diversity of structures that have yet to be fully explored, as most previous studies have focused on small numbers of topographic profiles of a few select structures.

Here, we develop a more comprehensive understanding of wrinkle ridges through a systematic analysis of the topography of a large population of structures on Mars. We have analyzed 265,092 profiles of 1585 compressional tectonic structures in the western hemisphere of Mars. Each ridge is characterized using its average topographic profile. The full population of ridges was then evaluated to identify distinct sub-types of wrinkle ridges. Representative structures were then chosen for inversion of the topographic profiles to constrain the underlying geometry of faults.

Classification methods. Wrinkle ridges were subdivided into linear segments using the mapping of Knapmeyer [6]. Ridges were evaluated using detrended gridded MOLA topography. Topographic profiles were taken perpendicular to each segment with a spacing of 463 m. For each ridge, individual profiles were shifted and aligned by maximizing the correlation with the average profile. Surfaces in which the topography was dominated by unrelated structures (e.g., impact craters) were removed by excluding all points more than 1.5 standard deviations from the mean at each location in the profile. The aligned profiles were then averaged for each wrinkle ridge. The endpoints of the wrinkle ridge in each average profile were selected manually. Any average profiles dominated by topographic structures other than the wrinkle ridge of interest were rejected, leaving 715 structures. Ridges were oriented with the steeper side facing to the right in each profile, aligned at the location of maximum height, and normalized in elevation relative to the ridge height and in distance relative to the ridge width. The average profiles were then evaluated using a *K-means* unsupervised classification algorithm. The population of compressional tectonic structures was initially subdivided into 12 classes. Duplicate classes with similar properties were identified by visual inspection and combined.

Classification results: Wrinkle ridges cluster into 3 main morphological groups:

1) Asymmetric concave upward ramps with a relatively uniform concavity on the gently sloping back-limb ("ramp", n=173).
2) Ridges consisting of primary and secondary antiforms consistent with the presence of a secondary back-thrust [7] ("double", n=187)
3) Quasi-symmetric ridges in which the peak ridge height is nearly centered within the structure ("symmetric", n=355).

The clustering of profiles into classes is imperfect, with many structures in one class sharing characteristics with those of another. Nevertheless, results are largely confirmed by visual inspection. Regionally, all classes are represented in most areas, though some local clustering is found (Fig. 1). Characteristics of the profiles (Fig. 2) are discussed below.

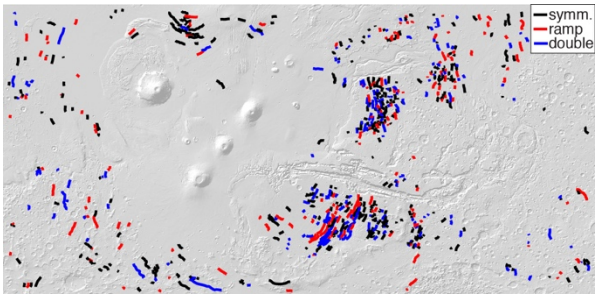

Figure 1. Distribution of wrinkle ridges classified into the three sub-groups (map extends from 180-360°E, 44°S-44°N).

Topographic step across the structures: One important question with respect to wrinkle ridge tectonics is whether wrinkle ridges exhibit a discrete topographic step indicative of an offset across a deeply penetrating thrust fault [4] or not [5]. For the ramp and double ridges with topographic steps >10% of the ridge height, upward steps (n=104) and downward steps (n=183) in the direction of fault vergence were both common. While individual examples may appear to support a topographic step downward in the direction of fault vergence, this is weakly supported by the population as a whole. These results support tectonic models in which faulting is confined to shallow depths within the crust.

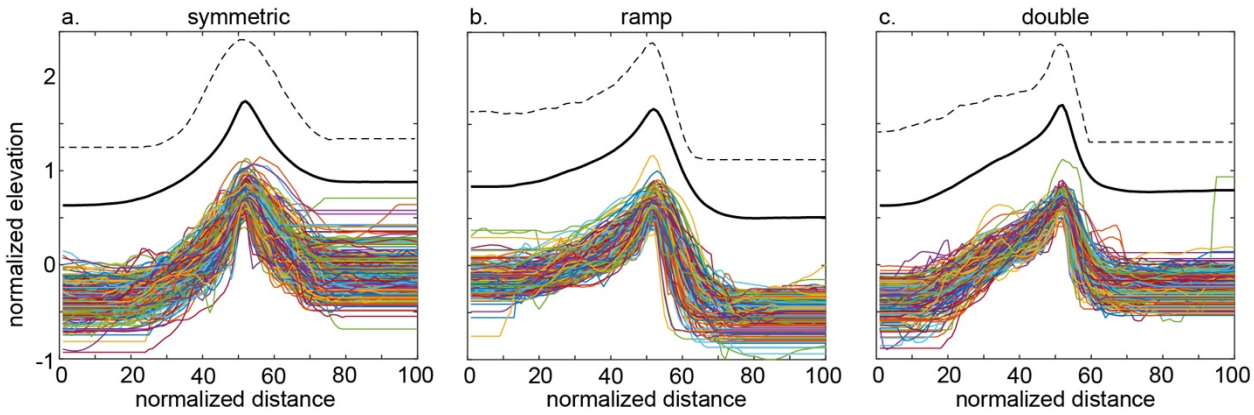

Figure 2. Individual profiles (colored lines), average profile (bold black line), and a single representative profile (dashed line) for wrinkle ridges in the three classes identified: symmetric (a), ramp (b), and double (c).

Secondary antiforms: The presence of a secondary antiform has been interpreted as evidence of a backthrust fault [7]. The double ridges, comprising 26% of the population, exhibit such secondary antiforms supporting the presence of backthrusts. Some of ridges classified into the ramp and symmetric groups also show a similar but less pronounced pattern.

Symmetric vs asymmetric structures: Thrust faults are expected to generate highly asymmetric structures. Nevertheless, a large fraction (40%) of structures analyzed in this study are largely symmetric. While many of the structures classified in the symmetric group show clear but subtle asymmetries in the individual average profiles, a large number are highly symmetric. Such symmetric structures could be brought about by two symmetric but antithetic thrust faults generating a pop-up structure. The continuum of forms suggests that this structure may be a variation on the thrust-backthrust architecture that characterizes many wrinkle ridges.

Inversion: One average profile of a typical double ridge exhibiting primary and secondary antiforms was selected for further analysis. The profile was inverted using a Monte Carlo approach, coupled with a boundary element model [8] including a listric master thrust fault, a backthrust fault, and layer parallel shear at a weak horizon. This model yielded best-fit parameters (and 1-σ range) for the master fault dip of 19° (16-25°) extending from 2.1 km (1.9-2.5 km) to 9.7 km (7.0-12.3 km) in depth (Fig. 3). The backthrust fault exhibited a dip of 26° (21-35°), extending from a depth of 0.9 km (0.4-1.3 km) to its intersection with the primary thrust at a depth of 2.4 km (2.0-2.9 km). However, we note a secondary minimum in the solution space which fits the profile nearly as well with a listric master fault extending to within 1.5 km of the surface, demonstrating the importance of a thorough investigation of the parameter space. The low fault dip is consistent with the measured dip of a wrinkle ridge fault exposed in outcrop [9].

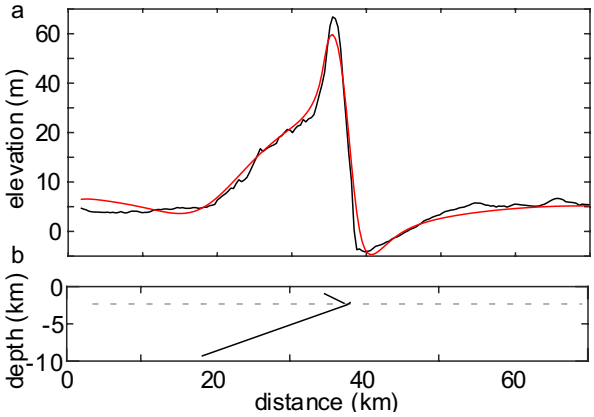

Figure 3. a Average ridge profile (black) and best-fit model (red), and **b** corresponding geometry of thrust faults (black) and layer-parallel slip surface (dashed).

Summary and discussion: Wrinkle ridges exhibit a wide diversity of forms, including concave upward ramps, structures with primary and secondary antiforms, and symmetric structures. All types are found on all surfaces. The population as a whole does not support the presence of a topographic step across the ridge, favoring shallow thrust faults. Inversions of the double ridges reveal the importance of backthrusts and layer-parallel slip in achieving the observed topography. The low fault dip indicates greater contraction across the structures than is commonly assumed.

References: [1] Bouley, S. et al., (2018), *EPSL, 488*, 126–133. [2] Watters, T. R., (1993), *JGR, 98*, 49–60. [3] Schultz, R. A., (2000), *JGR, 105*, 12,035-12,052. [4] Golombek, M. P. et al., (2001), *JGR, 106*, 23811-23821. [5] Watters, T. R., (2004), *Icarus*, *171*, 284–294. [6] Knapmeyer, M. et al., (2006), *JGR, 111*, E11006, doi:10.1029/2006JE002708 (2006). [7] Okubo C. H and R.A. Schultz, (2004), *GSA, 116*, 594–605. [8] Crouch, S. L. and A. M. Starfield, (1983). [9] Cole, H. M. and J. C. Andrews-Hanna, (2017), *JGR, 122*, 889–900, doi:10.1002/2017JE005274.